

# Dynamic Localized Autonomous Chaotic Orbital Patterns from Rotation-Translation Sequences



Bernd Binder

**Abstract** Consider an ordered sequence of repeated operations given by a distance-dependent rotation followed by a translation. Operating this sequence with special parameters and initial conditions provides for characteristic spatial density patterns in the plane. In this work we introduce an additional orbital rotation and find local chaotic orbital patterns and attractors in the plane. There are two ways to form a local density from discrete long-range jumps: either a jump-back boundary condition or rotating the jump direction. We focus on real time simulations, where the chaotic evolution and vivid dynamics (the live cycles of orbitals) with characteristic numbers or stability conditions is manifest. Ring bifurcations, stable and unstable chaotic orbital patterns or solitons emerge dynamically with start conditions and without any “hard” additional boundary or radial back-jump-condition. We show some typical orbital patterns and suggest a method of categorization.

**Keywords** Chaos · Rotation · Bifurcation · Discrete · Translation · Reflection · Closed loop · Orbit · Soliton · Wavelet · Quantum · Attractor · Pattern · Sequence · Simulation · Commutation · Operator · Geometric phase · Magic angle · Spiral · Ray

## 1 Introduction

Repeating a discrete sequence of rotation—translation—reflection operations can provide for a wide range of interesting and very complex pattern emerging from chaotic jumps, see Skiadas [1–3]. Counterintuitively, discrete long-range jumps often follow a continuous type of flow pattern, e.g. in [3] very similar to v. Kármán Streets, see Fig. 1.

To get a special pattern requires adjusting the rotation strength parameter and eventually a boundary distance condition parallel to the jump direction. We found that the correspondent pattern building process can be assigned to small nonlinear

---

B. Binder (✉)  
89182 Bernstadt, Germany  
e-mail: [bernd@binders.de](mailto:bernd@binders.de)

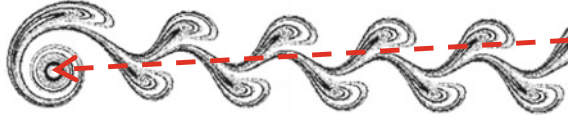


**Fig. 1** Skiadis type v. Kármán Streets with rotation parameter  $c_1 = \pi$ , power exponent  $p_1 = -2$ , reflection  $m = 2$ , and long jump back (red arrow)

geometric (phase) shifts arising in the rotation-translation sequence on every loop Binder [4, 5]. Applying this nonlinear concept it is possible to generate a broad range of patterns, including periodic structures like waves, circles, saw-tooth or point-like discrete geometries by desktop computer simulations. The model can be generalized to multiple rotation-translation sequences on orthogonal rotation axes in higher dimensions Binder [5].

In this work we add to the basic rotation-translation-reflection model an extra orbital rotation orthogonal to the jump direction and wonder, if we can generate in these ways structures on closed orbits. This means, we add another rotation around the existing singularity (at the origin) and look for orbital structures. As a result, we find chaotic periodic structures emerging on the orbit without any additional constraint like a jump-back condition limit. These dynamical structures are more or less stable and show an internal dynamics sometimes like a vivid entity. In this paper we point to some interesting patterns/simulations and try to make a categorization according to boundary conditions and characteristic parameter.

## 2 The Basic Operation Sequence

In the plane the chaotic model is based on a discrete iteration sequence of the polar vector

$$\vec{r} = \begin{pmatrix} x \\ y \end{pmatrix}. \quad (1)$$

Its polar coordinates are given by the radius  $r = |\vec{r}|$  and polar angle/direction  $\varphi$ , where

$$x = r \sin \varphi; \quad r^2 = x^2 + y^2; \quad \varphi = \arctan 2(x, y). \quad (2)$$

The iteration will be given by an ordered sequence composed by the two or three operations given by a polar **rotation R** and non-radial **translation T** and eventually a radial **inversion I**. The vector coordinate evolves in successive operations within one iteration sequence with numbering  $t \rightarrow t + 1$  according to

$$\vec{r}_t \rightarrow \vec{r}_R \rightarrow \vec{r}_T \rightarrow \vec{r}_I = \vec{r}_{t+1}$$

by the following relations:

- I. A radius dependent polar/central **rotation** including **reflection**

$$\vec{r}_R = \mathbf{R}(\vec{r}, \Delta\phi). \quad (3)$$

with rotation angle  $\Delta\phi$  in (3) composed by the following rotation and reflection components

$$\Delta\phi = \Delta\phi_1 + \Delta\phi_2 \quad (4)$$

given by:

1.  $\Delta\phi_1$  in (4) is the Skiadas type rotation angle that has a power-law radial distance dependence with exponent  $p_1 < 0$

$$\Delta\phi_1 = c_1 r^{p_1}, \quad (5)$$

2.  $\Delta\phi_2$  in (4) generalizes the reflection given by the difference  $\sigma - \varphi$  multiplied by a reflection mode  $m$

$$\Delta\phi_2 = m(\sigma - \varphi), \quad (6)$$

where  $m = 2$  is a reflection to the opposite side with respect to the initial polar angle  $\varphi$  in the co-rotating frame. In our special case, the global direction  $\sigma$  in (6) sums up with a constant orbital rotation  $c_0$  eventually driven by a radial power-law  $c_2 r^{p_2}$

$$\sigma = \sigma_t = \sigma_{t-1} + c_0 + c_2 r^{p_2}. \quad (7)$$

The total rotation is with in (4)–(7) given by

$$\Delta\phi = c_1 r^{p_1} + m(\sigma - \varphi), \quad (8)$$

and the rotation in (3) provides for the new orientation angle

$$\varphi_R = \varphi + \Delta\phi. \quad (9)$$

- II. The non-radial **translation**  $\vec{r}_T = \mathbf{T}(\vec{r}_R, \varphi, \Delta r) = \mathbf{T}(\vec{r}_R, \vec{\Delta r})$  of the rotated  $\vec{r}_R$  by a translation shift  $\vec{\Delta r}$

$$\vec{r}_T = \mathbf{T}(\vec{r}_R, \vec{\Delta r}) = \vec{r}_R + \vec{\Delta r} \quad (10)$$

in the initial  $\varphi$ —direction (and not in the actual  $\varphi_R$ —direction of (9)) where the polar component of the translation in (10) are given by

$$\vec{\Delta r} = \pm \begin{pmatrix} \Delta x \\ \Delta y \end{pmatrix} = \pm |\vec{\Delta r}| \begin{pmatrix} \cos \\ \sin \end{pmatrix} = c_3 r^{p_3} \begin{pmatrix} \cos \varphi \\ \sin \varphi \end{pmatrix}, \quad (11)$$

Equation (11) generalizes the usual “jump” in  $x$ —direction [1–3], where the unit jump has  $|\vec{\Delta r}| = 1$  or always  $c_3 = \pm 1$  with  $p_3 = 0$ . In this paper we will consider for simplicity only unit jumps and in Chap. 7 negative jumps with  $c_3 = -1$ .

- III. Finally there could be an additional **inversion** operation with respect to the origin

$$\vec{r}_I = \mathbf{I}(\vec{r}_T) = \vec{r}_T / |\vec{r}_T|^2, \quad (12)$$

with invariant direction angle but inverse length to get a rotation-translation-inversion sequence. This inversion could also be used as a method to jump back near to the rotation singularity.

### 3 Categories of Jumping Patterns

Without orbital rotation the jumps would only go in one direction (usually the  $x$ -direction) and disappear to infinity. There are two ways to form a local density: either a jump-back boundary condition or rotating the jump direction. The v. Kármán Street pattern in Figs. 1 and 2 and the typical  $2d$  wave pattern on the plane in Fig. 3 have a jump-back distance condition in the  $x$ -direction, which means, if the distance to the origin in jump direction exceeds a limit, a jump back near to the origin follows (Figs. 4 and 5).

With a new extra orbital rotation orthogonal to the jump direction we get local chaotic patterns without any orbital conditions (no jump condition) similar to the orbital solutions we know from quantum mechanics. We will call them “Localized Autonomous Chaotic Orbital Patterns” or LACOP, where we get many interesting orbital structures for integral  $p_1, p_2, m$ . It makes sense to group the jumping patterns according to the boundary conditions, where we have identified five categories given by:

1. **random starts condition:** long jump back (red arrow) randomly near to center, if distance or number of jumps exceeds a limit (see examples in Figs. 1, 2, 6 and 7).
2. **periodic boundary condition:** a defined long jump back to the back side, if distance exceeds a limit  $R_{\max}$ , see Fig. 3.
3. **inversion condition:** inversion operation  $\vec{r}' = \vec{r}/r^2$  if distance  $r$  exceeds a limit  $R_{\max}$ , see (12).

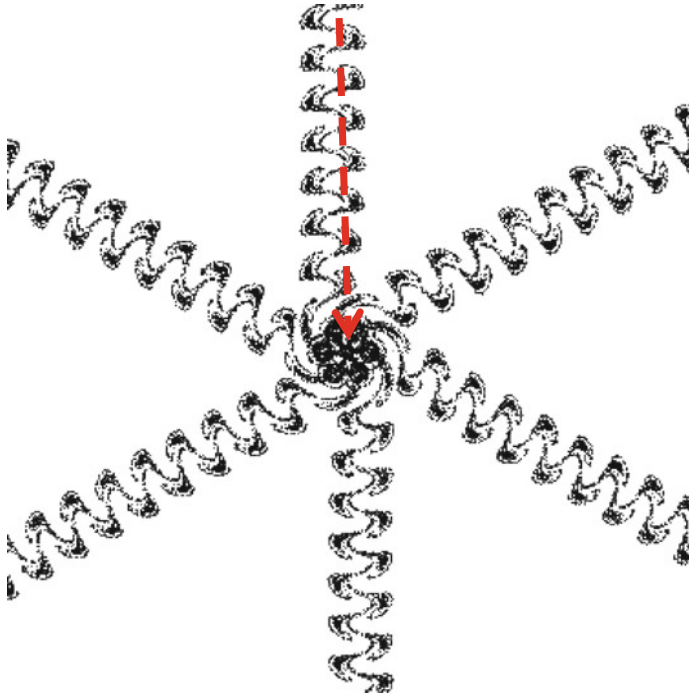


**Fig. 2** Long jump back with 6 arm-symmetric v. Kármán Street pattern,  $c_2 = 2\pi/6$ , with  $m = 2$ ,  $c_1 = \pi$ ,  $p_1 = -2$ , and  $p_2 = 0$

**Fig. 3** Periodic boundary jump back conditions producing waves, where  $p_1 < 0$ ,  $p_2 = 0$ ,  $m = 2$

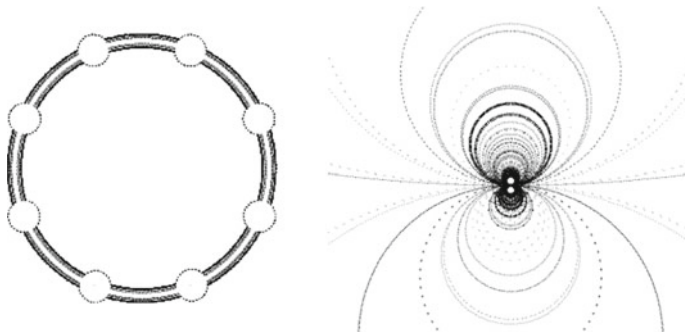
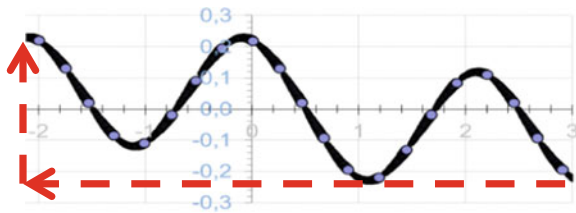


**Fig. 4**  $p_1 = p_2 - 1$  with  $p_2 = 2$ , left: LACOP with  $m = 1$ , right: random starts with  $m = 2$  dipole

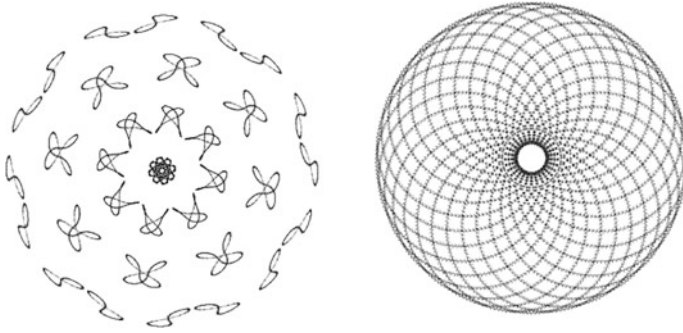


**Fig. 5** LACOP with regular orbital structure, examples of patterns with  $m = 0$ ,  $p_1 = 0$ ,  $p_2 = -1$ ,  $p_3 = 0$ .

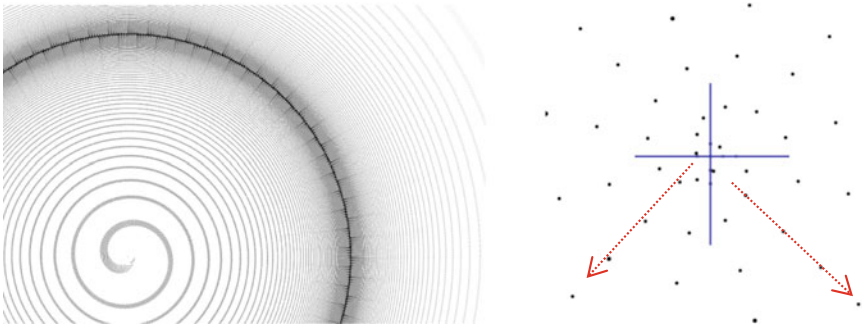


**Fig. 6** Radial rays intersecting spirals according to (13) and (14), left:  $m = 1$ ,  $c_3 = -1$ ,  $p_1 = 0$ ,  $p_2 = 1$ ,  $M > 100$ ,  $J = 0.5$ , right:  $m = 1$ ,  $c_3 = 1$ ,  $p_1 = -2$ ,  $p_2 = 0$ ,  $M = 5$ ,  $J = 0.5$

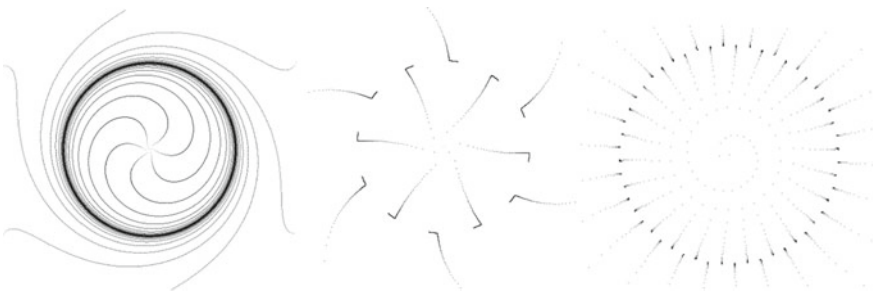


**Fig. 7** Linear rays for  $m = 1$ ,  $c_3 = -1$ ,  $p_1 = 0$ ,  $p_2 = 1$  left and mid  $M = 3$ , right  $M = 13$ ,  $g = 0.001$

4. **no boundary condition:** rotated jumps around the center according to orbital quantum numbers and symmetries producing LACOP.
5. **parameter conditions:** relating the two parameter  $c_1, c_2$  can define a family of patterns, e.g., if we define a small isotropic geometric phase shift gap  $g = 1/N \ll 1$  and relating the coefficients via the geometric jumping gap  $g$  geometrically to the rotation-translation parameter according to

$$c_1 = \arccos(1 - g), \quad c_2 = 2\pi Jg. \quad (13)$$

In this case we get with  $= 1, 2, 3 \dots = 1/g, c_3 = -1, p_1 = 0, p_2 = 1$  special radial conditions like spirals intersected radial rays, see Figs. 6 and 7 with random starts near to the center (condition 1).

## 4 Physics Relevance

It is interesting comparing these structures to Quantum Electrodynamics and spin symmetries. The parameter conditions categories 5 and 6 of Chap. 3 can be combined with condition categories 1, 2, 3, 4, where  $p_2 = -1$  with  $m$ -pole provides for multipole type orbital ring clouds and field structures:

## 5 Simple $m = 0$ LACOP

Both regular and highly non-linear or chaotic are the  $m = 0$  patterns in a wide parameter range, see Fig. 5.

## 6 Monopole $m = 1$ Negative Jumps $c_3 = -1$ with Random Start Near to Center

Both, highly chaotic and regular are the  $m = 1, c_3 = -1$  patterns in a wide parameter range, see Figs. 6 and 7, where the geometric gap condition in (13) produces radial rays intersecting spirals with random starts. It is not surprising to get Fresnel Charge structures in Fig. 6 for  $p_2 = 1$ , since a Fresnel spiral has an inherent spiraling angular structure with  $\varphi \propto \sum \sigma \propto r^{p_2+1} = r^2$ .

With a second constraint between the two parameters  $c_1, c_2$  in addition to (13) given by the linear relation

$$Mc_1 = 2\pi J - c_2, \quad (14)$$

we get fixed points for the parameters recovering the magic angle condition  $M_{c_1} = \pm J \cos(c_1)$  Binder [5] with charge  $J$  and discrete points solutions, where spirals intersect for  $m = 1$  rays with center offset, see Figs. 6 and 7.

## 7 More Complex Vivid $m = 2$ LACOP

Very interesting and exciting is the chaotic dynamics of the  $m = 2$  LACOP orbitals, see Fig. 8 and some mixed examples in Fig. 9. There is in most cases no static or stationary solution, since the orbitals often show a chaotic variation in the orientation or orbital shape. Therefore, a stable LACOP should be properly initialized; usually by an high enough orbital rotation parameter  $c_2$  (spin, energy) while increasing the  $m$ -parameter from 1 to 2. In simulations the solutions (recorded as videos) appear to be like vivid orbitals with inherent chaotic dynamics especially in the substructure of orbital rings:

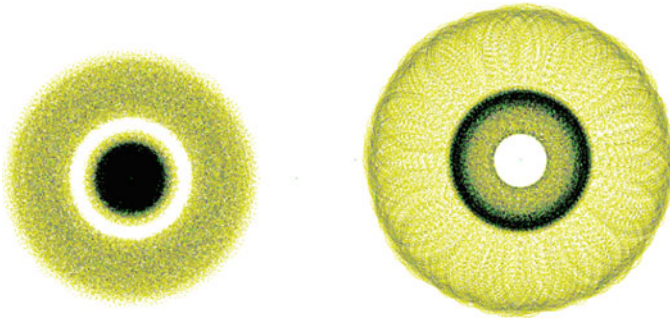


**Fig. 8** Vivid pulsating LACOP with different orbital structure expanding and contracting (the two examples are snapshots from the same LACOP) with  $m = 2$ ,  $p_1 = -2$ ,  $p_2 = 0$ ,  $p_3 = 0$ ,  $c_1 \approx -0.02035\pi$ ,  $c_2 \approx 1.0021\pi$

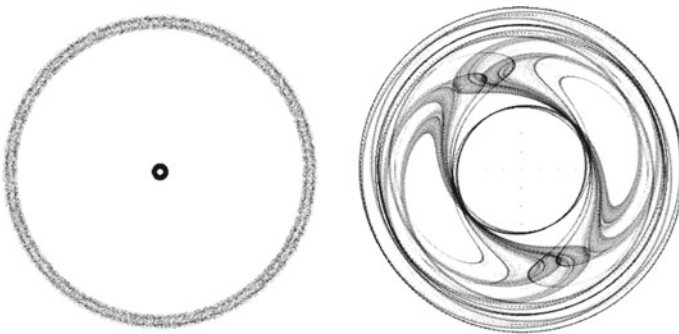


**Fig. 9** Typical chaotic LACOPs with a core and a hole in the center  $p_1 < p_2$ ,  $m > 0$





**Fig. 10** Radial ring orbit bifurcation  $p_1 = -1$ ,  $m = 1$ , left: 4th bifurcation with 16 orbits where  $c_1 \cong 1.657\pi$ , right: chaos starting at  $c_1 \cong 1.65\pi$

## 8 Orbital Bifurcations for $m = 1$ LACOP

Under special conditions, the radial distribution of orbits shows a bifurcation tree, see Fig. 10.

## 9 Conclusion

The resulting patterns often show a localized ring shape with several mixed orbits in a kind of hydrodynamic-type orbital shelf flow and an empty region or hole at the center.  $m$ —poles or reflection modes with higher  $m$  show more complex and unstable pattern. A stable form must be initialized; otherwise the pattern collapses or expands to infinity. The emerging LACOP solitons or fixed point solutions are having always characteristic.

- special parameter  $m$ ,  $c_i$ ,  $p_i$ , where usually  $p_1 \leq 0$ ,  $p_2$  and  $p_3 \geq 0$ , see Table 1.
- nonlinear structure, chaotic dynamics, bifurcations, and fluctuations
- radial and orbital wave numbers
- radial and orbital symmetries
- geometric phase conditions
- fixed point sets (i.e., two magic conditions (13) and (14) with numbers  $J$ ,  $M$ )

Finally, we propose that this computer experiments show some relevance to quantum physical systems since we have

- a wave attractor showing quantization effects in terms of rotational units,
- a quantization of monopole and multipole charges,
- a basic non-zero quantum spin in the two main operators (rotation-translation, non-commutative) with characteristic geometric phase shifts,
- point-like local events with emerging global wave-like probabilistic patterns.

**Table 1** Small LACOP exponent combinations

“Jump back” needed?	$p_1$	$p_2$	$p_3$	$m$	$c_3$
Yes	-2	0	0	>0	1
No	-2	0	0	>0	1
No	-1	1	0	>-1	1
No	-1	2	0	>1	1
No	-1	2	1	>0	1
No	0	1	0	1	-1
No	0	1	0	>1	1
No	0	2	0	>1	1

There will be videos of simulations available on the internet with title “Dynamic Autonomous Chaotic Orbital Patterns” or tag “#DACOPSimulation”.

## References

1. C.H. Skiadas, C. Skiadas, Chaos in Simple Rotation-Translation Models, nlin.CD. (2007) <http://arxiv.org/abs/nlin/0701012v1>
2. C.H. Skiadas, C. Skiadas, *Chaotic Modeling and Simulation: Analysis of Chaotic Models, Attractors and Forms* (Taylor and Francis/CRC, London, 2008)
3. C.H. Skiadas, Von Karman Streets chaotic simulation, in *Topics on Chaotic Systems*, ed. by C.H. Skiadas, I. Dimotikalis, C. Skiadas (World Scientific, 2009), pp. 309–313
4. B. Binder, Magic angle chaotic precession, in *Topics on Chaotic Systems: Selected Papers from CHAOS 2008 International Conference*, Singapore (World Scientific Books, 2008), pp. 31–42
5. B. Binder, Chaotic modelling and simulation: rotations-expansion-reflections chaotic modelling with singularities in higher dimensions. *Chaotic Modeling and Simulation (CMSIM)* **1**, 89–106 (2013)